Molecular Crystals and Liquid Crystals

Publication details, including instructions for authors and subscription information:
http://www.tandfonline.com/loi/gmcl20

Synthesis and Optical Nonlinearities of a 2-Amino-1,2,3-triazolquinone Derivative

G. Ramos-Ortiz [a], S. Romero-Servin [a], J. L. Maldonado [a], M. A. Meneses-Nava [a], O. Barbosa-García [a], P. Zapata Castillo [b], M. A. Méndez-Rojas [b] & Herbert Höpfl [c]

[a] Centro de Investigaciones en Óptica, León, Guanajuato, México

[b] Departamento de Ciencias Químico-Biológicas, Universidad de las Américas, Puebla, San Andrés Cholula, Puebla, México

[c] Centro de Investigaciones Químicas, Universidad Autónoma del Estado de Morelos, Cuernavaca, Morelos, México

Version of record first published: 17 Dec 2009

To cite this article: G. Ramos-Ortiz, S. Romero-Servin, J. L. Maldonado, M. A. Meneses-Nava, O. Barbosa-García, P. Zapata Castillo, M. A. Méndez-Rojas & Herbert Höpfl (2009): Synthesis and Optical Nonlinearities of a 2-Amino-1,2,3-triazolquinone Derivative, Molecular Crystals and Liquid Crystals, 515:1, 109-124

To link to this article: http://dx.doi.org/10.1080/15421400903291228

Mol. Cryst. Liq. Cryst., Vol. 515, pp. 109–124, 2009

ISSN: 1542-1406 print/1563-5287 online
DOI: 10.1080/15421400903291228

Taylor & Francis
Taylor & Francis Group

Synthesis and Optical Nonlinearities of a 2-Amino-1,2,3-triazolquinone Derivative

G. Ramos-Ortiz[1], S. Romero-Servin[1], J. L. Maldonado[1], M. A. Meneses-Nava[1], O. Barbosa-García[1], P. Zapata Castillo[2], M. A. Méndez-Rojas[2], and Herbert Höpfl[3]
[1]Centro de Investigaciones en Óptica, León, Guanajuato, México
[2]Departamento de Ciencias Químico-Biológicas, Universidad de las Américas, Puebla, San Andrés Cholula, Puebla, México
[3]Centro de Investigaciones Químicas, Universidad Autónoma del Estado de Morelos, Cuernavaca, Morelos, México

We report on the synthesis and nonlinear optical characterization of a novel 2-amino-1,2,3-triazolquinone derivative, namely, 2-(yliminopropylphenyl-N,N′-dimethylamino)naphto-1,2,3-triazole-4,9-dione (ATZQ). The second-order nonlinear optical properties in solution were characterized using the hyper-Rayleigh scattering (HRS) technique, while the third-order nonlinearities of ATZQ-doped polymer films were measured through the use of the THG-Maker fringes technique. These experiments showed that this compound exhibits large second- and third-order nonlinear effects at the molecular level, with a first hyperpolarizability constant of $\beta \sim 834 \times 10^{-30}$ *esu at 1064 nm and a second hyperpolarizability constant of* $\gamma \sim 3.5 \times 10^{-33}$ *esu at the telecommunication wavelength range of 1200–1700 nm.*

Keywords: hyper-rayleigh scattering; nonlinear optics; quinone; SHG; THG; triazole

INTRODUCTION

The development of new organic materials possessing large nonlinear optical (NLO) properties have been intensively investigated for potential applications in photonic-based technologies, such as optical memories, electro-optical and all-optical switches, dynamic holography, and broadband optical telecommunications [1–4]. The large nonlinearities exhibited by π-conjugated molecules and polymers

Address correspondence to G. Ramos-Ortiz, Centro de Investigaciones en Óptica A.P. 1-948, 37000, León, Guanajuato, México. E-mail: garamoso@cio.mx

combined with their ultrafast response are ideal for the realization of these applications. Second-order NLO materials, for instance, are of interest for their application in high-speed electro-optic modulators and switches, while third-order compounds are promising for all-optical switching, optical computing, as well as optical limiting.

In the search of materials with large nonlinearities a wide variety of compounds have been studied, including dyes, π-conjugated polymers, charge-transfer complexes, organometallic compounds, etc. [5–10]. Organic donor or acceptor groups used in the design of NLO-phores such as pyrroles [11], nitrogen and oxygen donor containing aromatic rings [12], pyridinium salts [13,14], tetrathiafulvalenes [15,16] and pyridine N-oxides [17] have been investigated by several groups worldwide.

For the development of NLO materials, however, triazole derivatives, in particular 1,2,3-triazoles substituted at the 2-position, are compounds that have received much less attention. The most obvious explanation is the lack of a general synthetic procedure for the synthesis of 2-amino-1,2,3-triazoles. This contrasts with the fact that numerous studies have been carried out on the design of novel architectures for 1-substituted triazole derivatives and 1,2,4-triazoles, many of them having applications in medicine and biology [18–21]. Recently, a variety of 2-(triarylphosphazene)-1,2,3-triazolequinones have been prepared [22–25], while the nonlinear response in derivatives of 1,2,3- and 1,2,4- triazole systems have been explored. For instance, the 2-(yliminomethylphenyl-N,N′-diethylamino)- and a 2-(yliminomethylferrocenyl)-naphto-1,2,3-triazole-4,9-dione derivatives (see compounds 1 and 2 in Fig. 1) showed significant third-order NLO properties when excited with picosecond pulses near resonance [26–29]. The triazole ring inherent in all these compounds is chemically and thermally stable and is compatible with a wide variety of functional groups giving extended π-conjugated systems.

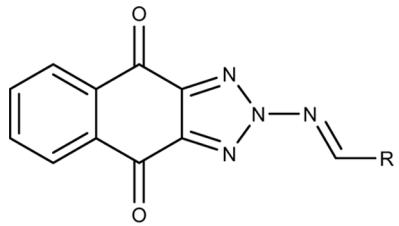

R = -C_6H_4-pNEt_2 (1), Ferrocenyl (2)

FIGURE 1 2-(yliminomethylphenyl-N,N′-diethylamino)-naphto-1,2,3-triazole-4,9-dione (**1**) and 2-(yliminomethylferrocenyl)-naphto-1,2,3-triazole-4,9-dione (**2**).

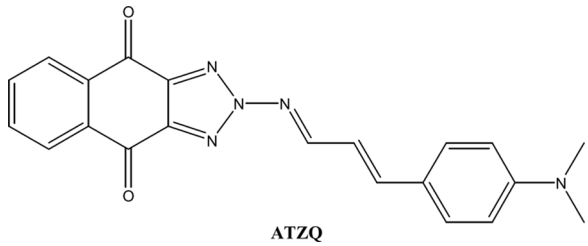

ATZQ

FIGURE 2 ATZQ.

On the other hand, 1,2,3 triazole isomers have been also used for the synthesis of quadrupolar and branched structures with strong two-photon absorption and optical limiting [30], while for the same purpose 1,2,4 triazole units were used in functionalized platinum acetylides [31] and for designing components for organic light emitting diodes (OLED) [32]. The latter moiety has also been used in crystals with second-order nonlinear activity [33,34].

To further explore the nonlinearities of compounds comprising triazole moeties, we synthesized a novel 2-amino-1,2,3-triazolquinone derivative, namely 2-(yliminopropylphenyl-N,N′-dimethylamino) naphto-1,2,3-triazole-4,9-dione (ATZQ) and examined its quadratic and cubic optical nonlinearities. In this compound (see Fig. 2), triazole and quinone moieties are combined to produce a small heterocyclic ring-system of coplanar conformation [29], which incorporates donor and acceptor groups to produce a *push–pull* π-conjugated system. The second-order nonlinear response of compound ATZQ at the molecular level was investigated using the hyper-Rayleigh scattering (HRS) technique. In addition, the third-order nonlinearities were also studied, in this case using the third-harmonic generation (THG) at the telecommunication wavelength range. It is worth to mention that both HRS and THG are techniques which involve the study of nonlinearities with electronic origin, thus the ultrafast response of ATZQ is reported.

2. EXPERIMENTAL

Materials and Equipment

All materials and solvents were used as received. NMR spectra were run on a Varian Mercury spectrometer at 200 MHz for ^{1}H, with tetramethylsilane (TMS) as an internal standard, using $CDCl_3$ as solvent. Melting points were determined using a Fischer-Johns apparatus. UV-Visible absorption spectra were recorded with a Varian Cary 100

spectrophotometer, in 1.0 cm quartz cells, at room temperature, in a range between 200 and 900 nm. IR spectra were recorded on a Varian 800 Scimitar FT-IR spectrometer at a spectral resolution of 4 cm^{-1} using an ATR accessory for finely grounded solid samples. High resolution mass spectra were obtained on a JEOL JMS 700 mass spectrometer. 2-(Triphenylphosphanylideneamino)naphtho-1,2,3-triazole-4,9-dione was prepared following a slightly modified procedure previously reported [28].

Synthesis of 2-(Yliminopropylphenyl-4-N,N′-dimethylamino)naphto-1,2,3-triazole-4,9-dione

To a solution of 2-(triphenylphosphanylideneamino)naphtho-1,2,3-triazole-4,9-dione (0.400 g, 1.870 mmol) in ethanol (30.0 mL), 0.327 g (1.866 mmol) of N,N′-dimethylcinnamaldehyde was added under stirring along with 100 μL of concentrated hydrochloric acid, and the mixture was refluxed overnight. The dark purple solid formed was separated by filtration, washed three times with cold ethanol, and dried at room temperature under vacuum. Yield 0.620 g (90%), m.p. 135–137°C. IR (cm^{-1}): 1679 (vs), 1560 (m), 1395 (m), 1355(m), 1222 (s), 1150 (m), 1015 (m), 974 (m), 720 (m). ^1H NMR (ppm): 9.28 (d, 1 H), 8.33 (d, 2 H), 7.83 (d, 2 H), 7.48 (d, 2 H), 7.35 (s, H), 7.28 (s, H), 6.92 (d, 1 H), 6.68 (d, 1 H). MS (m/z, FAB^+): $C_{21}H_{18}O_2N_5$, 372.14 (98.2, $[M+H]^+$), 289, 219, 154, 136, 107, 89, 77, 65, 51. UV-Vis ($CHCl_3$) $\lambda_{max} = 465$ nm.

X-Ray Crystallography

X-ray quality crystals (black plates) were grown from a DMF solution by slow evaporation. The data were collected at 100 K on a BRUKER-AXS APEX diffractometer equipped with a CCD area detector (Mo $K_\alpha = 0.71073$ Å, monochromator: graphite). Frames were collected via ω- and φ-rotation at 10 s per frame (SMART) [35]. The measured intensities were reduced to F^2 and corrected for absorption with SADABS (SAINT-NT) [36]. Structure solution, refinement, and data output were carried out with the SHELXTL-NT program package [37]. Non-hydrogen atoms were refined anisotropically. All data were corrected for Lorentz and polarization effects. C-H hydrogen atoms were placed in geometrically calculated positions using a riding model. All additional treatments were done through the WIN-GX; the corresponding molecular graphs were prepared with the ORTEP 3 and Mercury 1.2 programs [38–40]. Crystallographic data for ATZQ have been deposited at the Cambridge Crystallographic Data Center as

CCDC No. 692909. Copies of the data can be obtained free of charge upon application to CCDC, 12 Union Road, Cambridge CB2 1EZ, UK (E-mail: deposit@ccdc.cam.ac.uk).

SHG Measurements

The detection of incoherent second-harmonic generation (SHG) was employed to study the quadratic nonlinear response in ATZQ. In this case the SHG was detected using the HRS experimental configuration commonly described in the literature [41]. Briefly, the beam from a high-energy pulsed Nd-YAG laser (8 ns at the fundamental wavelength of 1064 nm, repetition rate of 10 Hz) was focused into a quartz cell of 4-cm path length by using a 30-cm focal-length lens. The cell contained chloroform solutions of ATZQ. A high-pass filter removed any visible light from the laser cavity. To efficiently collect the HRS signal at 90° we used a condenser system conformed by a large aperture aspheric lens ($f = 29.5$ cm, $\phi = 4$ cm) and a concave mirror ($f = 1.75$ cm, $\phi = 5.1$ cm). The collimated HRS light was then passed through a couple of low pass filters (Schott filters, KG5) to eliminate any scattered light at the fundamental frequency, and then focused to a photo-multiplier tube (PMT) using a 20-cm focal-length lens. A 3 nm FWHM interference filter centered at 532 nm was mounted at the entrance of the PMT. The HRS signals were detected and averaged by a digital oscilloscope. The experiment was computer controlled. To avoid optical breakdown, the solutions were filtered with 0.2 μm PTFE membrane filters and typical energies were set between 1 mJ and 4 mJ at the sample position.

TGH Measurements

The cubic nonlinearities were characterized by detecting the coherent THG from ATZQ-doped polymer films using the Maker-fringes experimental approach [42]. Briefly, the Nd-YAG laser described in SHG experiments pumped an optical parametric oscillator (OPO). The idler beam of this OPO was focused into the films with a 30-cm focal-length lens to form a spot with a radius of approximately 150 μm. The generated THG signal was separated from the pump beam using low pass filters (Schott filters, KG5) and detected with a PMT and a Lock-in amplifier. The THG measurements were performed for incident angles in the range from −40 to 40° with steps of 0.270 degrees. All experiments were computer controlled. For our purposes we used the tunability of the OPO within the wavelength range of 1200–1700 nm. Typical energies in our measurements were

set at 1 mJ per pulse at the sample position (corresponding to peak intensities of $\sim$0.18 GW/cm^2).

Preparation of ATQZ-Doped Polymer Films

To fabricate ATZQ-doped polymer films we dissolved polystyrene (PS) and compound ATZQ in a weight proportion of 70:30 wt% in chloroform as solvent. Then solid films were deposited on fused silica substrates (1 mm thick) using the spin coating technique with the following parameters: risetime of 3 s and 1200 rpm during 60 s. The obtained films had good optical quality showing negligible light scattering at visible and NIR wavelengths. The film thicknesses were measured with a surface profiler (Dektak 6 M, Veeco).

RESULTS AND DISCUSSION

Push-pull systems containing the 1,2,3-triazole moiety substituted at the 2-position are easily prepared by the method previously reported [28,29]. The 2-(triarylphosphanylideneamino)-1,2,3-triazole precursors can be hydrolyzed to the 2-amino-1,2,3-triazole derivatives. Both compounds react with aldehydes and unhindered ketones in polar solvents to generate the corresponding aza-Wittig or Schiff-base condensation products.

ATZQ is a molecule that possesses a donor-acceptor character as it is discussed later. There are only few reports on this class of NLO systems in which small heterocyclic rings are used as π-conjugated moieties [11–16]. Polyenes, oligophenylenes, and oligothiophenes are more commonly used for that purpose, whereby oligothiophenes are very efficient relays due to their rigid structure and coplanar conformation. The absorption spectra of ATZQ in solution and in spin-coated film are shown in Fig. 3. In this figure we see that a solution with a concentration of 100 μM of compound ATZQ produces an absorption band centered at 465 nm. This band is 30 nm red-shifted with respect to that exhibited by compounds 1 in Fig. 1, the latter compounds having a molecular structure similar to ATZQ but with a less extended π-conjugated bridge [26]. It is assumed that the absorption band in the visible part of the spectrum arises from an intramolecular electron-transfer process. On the other hand, when compound ATZQ is dispersed in a PS polymer film, this absorption band is centered at 457 nm.

Solvatochromism has been regarded as an indication of molecular nonlinearity in NLO chromophores, and it was used to evaluate 2-amino-1,2,3-triazolequinone systems [28,29]. Compound ATZQ shows λ_{max} values (wavelengths of absorption maximum) at 393 nm

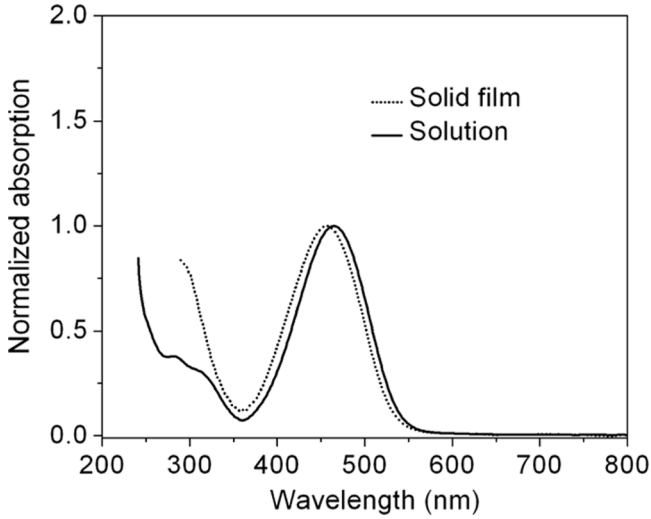

FIGURE 3 Absorption spectra for compound ATZQ in chloroform solution (concentration of 100 μM) and dispersed in a polystyrene film in a proportion of 30:70 wt%.

in dioxane (dielectric constant value, ε, 2.209), 465 nm in chloroform (ε, 4.806), 452 nm in THF (ε, 7.6), and 463 nm in DMF (ε, 36.7). The absorption maximum in this compound is red-shifted in polar solvents, indicating a strong solvatochromism. Solid-state X-ray analysis confirms the planarity of the extended conjugated π-system containing the quinone and the triazole. In fact, the π-systems attached to $-$N=R$-$ units usually adopt a coplanar conformation with respect to the rest of the molecule unless strong packing interactions are dominant [29]. In this case, the torsion angles along the conjugated π-system range from 0.5° to a maximum of 4° and indicate only a slight deviation from planarity. Therefore, the quinone-acceptor, the 1,2,3-triazole fragment and the cinnamaldehyde-donor moieties are located in the same plane, facilitating the intra-molecular electron transfer process, which is the most probable origin of nonlinearity [26]. Figure 4 is an ORTEP representation of ATZQ.

Geometry optimization and first principles theoretical calculation of the electronic structure of ATZQ carried out using the B3LYP exchange-correlation function [43] as implemented in the Gaussian 98 program package [44], together with a 6–31G(d) basis set was performed. The highest occupied molecular orbital (HOMO) and the lowest unoccupied molecular orbital (LUMO) are π and π^* combinations, respectively. The HOMO is mainly localized on the

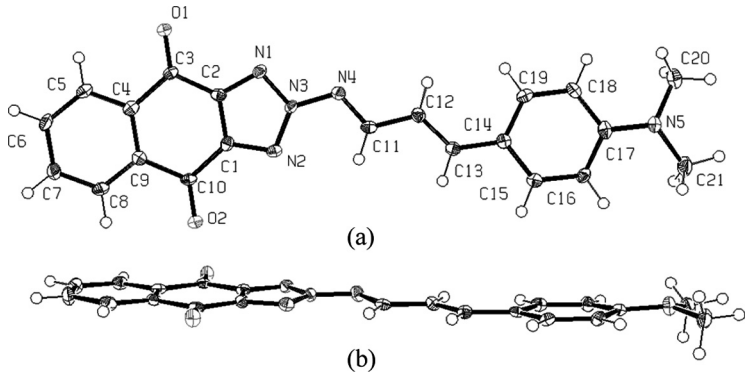

FIGURE 4 Atom labeling and thermal vibration ellipsoids (50% probability) for compound ATZQ.

3-(4-(dimethylamino)phenyl)-2-propenyl electron-donor fragment, while the LUMO is mainly localized on the naphtoquinone electron-acceptor fragment. It can be noticed that the 1,2,3-triazole moiety participates both in the HOMO and LUMO, working as a bridge between the donor and acceptor fragments (Fig. 5). The dipole moment was calculated to be 8.3 D.

Thus, as supported by the solvatochromic behavior and the crystal structure information, the conjugated backbone, including

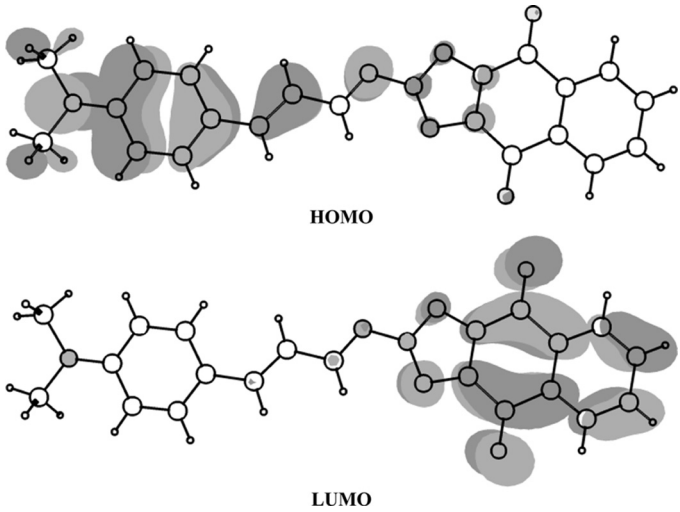

FIGURE 5 Frontier orbitals HOMO (a) and LUMO (b) for compound ATZQ.

the 1,2,3-triazole moiety, is mainly responsible for the intramolecular electronic transfer and, therefore, the nonlinear optical response.

HRS Experiments

The HRS signal was measured for solutions of ATZQ in chloroform using the external reference method to calculate its first hyperpolarizability β. For this purpose, *para*-nitroaniline (*p*-NA) dissolved in chloroform was employed as reference. In this method, the scattered second-harmonic signal is detected for a dilution series of ATZQ and for a dilutions series of *p*-NA. Both signals were then plotted as a function of molecular concentration such that the ratio of the two slopes (m and m_{pNA}) and the effective hyperpolarizabilities of ATZQ and *p*-NA are related by [41]:

$$\beta = \beta_{pNA}(m/m_{pNA})^{1/2}. \quad (1)$$

To calibrate the apparatus we also measured the HRS signal of the octupolar compound crystal violet (CV), whose nonlinearities were recently reported [45,46]. Figure 6 shows the second harmonic intensities of *p*-NA, CV and ATZQ at different molecular concentration. By using Eq. (1) with $\beta_{pNA} = 23 \times 10^{-30}$ esu [41] and with the slope of *p*-NA obtained from the fitting of data in Fig. 6a, the first hyperpolarizability of CV resulted in $\beta = 1328 \times 10^{-30}$ esu, which is in satisfactory agreement with the literature values [45,46]. Following the same procedure, the hyperpolarizability obtained for ATZQ was $\beta = 834 \times 10^{-30}$ esu. This value is relatively large when compared with

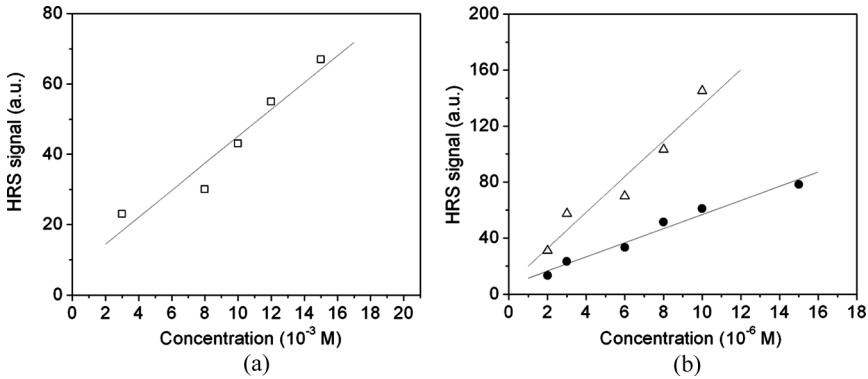

FIGURE 6 HRS intensity versus molecular concentration for a) *p*-NA, b) ATZQ (filled circles), and the octupolar molecule crystal violet (open triangles).

other molecules possessing dipolar moments. To verify that the measurements were not influenced by light emission induced by two-photon absorption, we also detected the fluorescence spectra of CV and ATZQ under direct laser excitation at 532 nm (8 ns pulses). The fluorescence was analyzed with a monochromator and a PMT system, while a notch filter was used to eliminate the scattered pump radiation, allowing to observe the fluorescence at the very near vicinity of 532 nm. Under this excitation conditions, compound ATZQ did not exhibit an appreciable fluorescence at any wavelength, while CV had a fluorescence band centered at 620 nm, which was far enough from the HRS wavelength so that it did not interfere with our measurements. It is well know that CV is a very poor fluorescent material, and here it was observed that ATZQ has an even weaker fluorescence emission.

Compound ATZQ also exhibited strong HRS under femtosecond (fs) excitation. Figure 7 shows the response of ATZQ when pumped by a train of 100 fs pulses at 800 nm with approximately 7 nJ/pulse and 80 MHz repetition rate (delivered by a Ti:Sapphire laser, model Tsunami 3941-M1S, Spectra Physics). This spectrum was easily detected with the use of a monochromator and detected with a PMT. The high repetition rate of the laser in combination with the high level of HRS signal from ATZQ allowed an easy detection by just using a lock-in amplifier. Note that the spectrum in Fig. 7 is centered at half

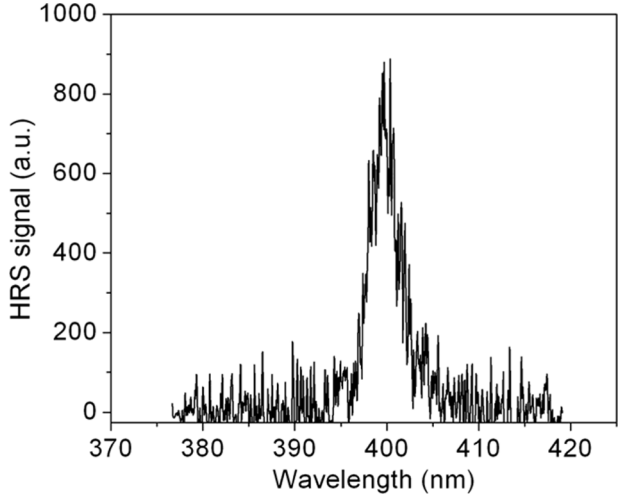

FIGURE 7 HRS spectrum of compound ATZQ with excitation at 800 nm.

of the excitation wavelength which is a clear evidence of the HRS effect. Furthermore, the narrow bandwidth (∼4 nm FWHM) was expected for a second-harmonic process generated by short pulses of 100 fs at 800 nm when the time-bandwidth product is considered for Fourier-transform-limited pulses. Thus, the high intensity observed for the HRS signal shows that ATZQ might also exhibit significant quadratic nonlinearities in the fs regime at 800 nm. In this case, however, we did not measure β for ATZQ as the sensitivity of our apparatus was below the signal generated by the reference molecule *p*-NA, while the HRS signal for CV at this particular wavelength was hindered by a fluorescence band induced by two-photon absorption, as it was previously reported [47] and confirmed in our experiments.

THG Experiments

In regard to cubic nonlinearities, Fig. 8 shown the third-harmonic signal generated by a 76-nm thick ATZQ-doped polystyrene film as a

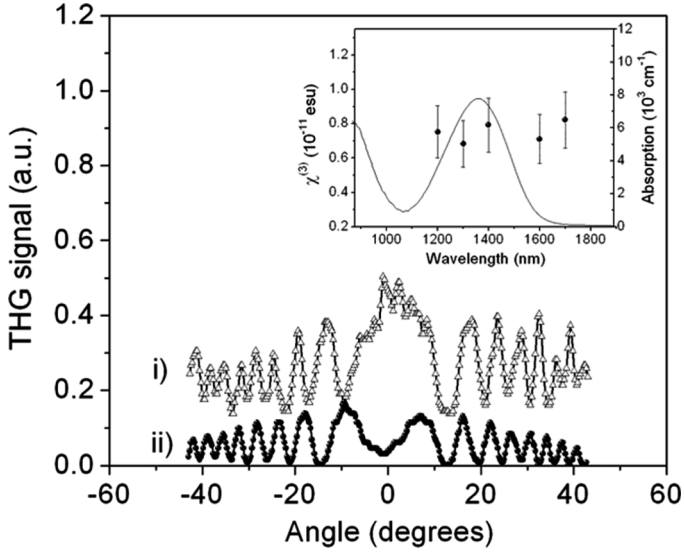

FIGURE 8 THG Maker-fringes patterns for i) a 76-nm-thick polymer film doped with 30 wt% of compound ATZQ; ii) a 1-mm-thick substrate without a polymer film deposited on it. The fundamental wavelength is 1200 nm. Inset: wavelength dependence of the third-order nonlinear susceptibility (left and bottom axes). The estimated errors in susceptibilities are indicated. As reference, the absorption spectrum (right and bottom axes) for the film is included with the wavelength multiplied by a factor of three.

function of the angle of incidence for the pump beam at the wavelength of 1200 nm. In this figure, the THG from a 1-mm-thick substrate is also included. In the Maker-fringes technique, the THG peak intensity $I^{3\omega}$ from the substrate-film structure is compared to that produced from the substrate alone. The nonlinear susceptibility $\chi^{(3)}$ in a film of thickness L_f is determined from [42]:

$$\chi^{(3)} = \chi_s^{(3)} \frac{2}{\pi} L_{c,s} \left(\frac{\alpha/2}{1 - \exp(-\alpha L_f/2)} \right) \left(\frac{I_f^{3\omega}}{I_s^{3\omega}} \right)^{1/2}, \tag{2}$$

where $\chi_s^{(3)}$ and $L_{c,s}$ are, respectively, the nonlinear susceptibility and coherence length for the substrate at the fundamental wavelength; α is the film absorption at the harmonic wavelength. Equation (2) is valid when the condition $L_f \ll L_{c,s}$ is satisfied. Thus, the ATZQ-doped polystyrene film with a doping level of 30% possesses a nonlinear susceptibility of $\chi^{(3)} = 0.75 \times 10^{-11}$ esu at 1200 nm. To perform the calculation using Eq. (2), we considered $\chi_s^{(3)} = 3.1 \times 10^{-14}$ esu, which is practically a constant for the range of wavelengths used in our experiments [48]. $L_{c,s}$ was obtained from tabulated refractive index values for fused silica. We point out that the nonlinear susceptibility did not exhibit significant variations when the excitation was tuned to longer wavelengths within the telecommunication band range, as it is shown in the inset of Fig. 8. To visualize multiphoton resonances the inset in Fig. 8 also shows the absorption curve for the film with the scale for the wavelength multiplied by a factor of 3. Here we observed that the nonlinearities are partially enhanced by three-photon resonances, even though $\chi^{(3)}$ did not exhibit a notorious dispersion. This lack of dispersion can be due to the fact that the film absorption is significantly smaller in comparison with polymer films doped with other organic molecules with large absorption and pronounced $\chi^{(3)}$ dispersion [49]. Therefore, at the telecommunication wavelength range of 1200–1700 nm the third-order nonlinear susceptibility of ATZQ polymer films was about 240 times larger than the value for fused silica. The macroscopic nonlinear susceptibility $\chi^{(3)}$ can be used to calculate the second hyperpolarizability γ, which is a molecular parameter of interest. The second hyperpolarizability is expressed as $<\gamma> = \chi^{(3)} / L^4 N_s$ where N_s is the density of molecules in the polymer films and $L = (n^2 + 2)/3$ is the correction factor due to local field effects with n being the refractive index. By assuming that the films have the refractive index and density of PS, and by using a molecular doping level of 30%, the calculated γ value for ATZQ is approximately 3560×10^{-36} esu within the wavelength range 1200–1700 nm.

TABLE 1 Optical Properties of Compound ATZQ

	Microscopic	Macroscopic
Dipole moment	$\mu = 8.3$ D (theoretical calculation)	—
Quadratic nonlinearities	$\beta = 834 \times 10^{-30}$ esu at 1064 nm	—
Cubic nonlinearities	$\gamma = 3560 \times 10^{-36}$ esu at 1200–1700 wavelength range	$\chi^{(3)} = 0.7 \times 10^{-11}$ esu at 1200–1700 wavelength range

In the following, we compare the nonlinearities of compound ATZQ (summarized in Table 1) to those exhibited by other efficient nonlinear molecule comprising triazol moieties. For instance, in core-modified phthalocyanines containing a 1,2,4-triazole moiety the hyperpolarizabilities measured at 1340 nm by HRS and THG were of the order of $\beta \sim 100 \times 10^{-30}$ esu and $\gamma \sim 10^{-33}$ esu, respectively [50]. Then, ATZQ has a first hyperpolarizability approximately eight times larger than the triazolephthalocyanine, while their second hyperpolarizabilities are about the same. Recently, the group of Rangel-Rojo et al. have reported the nonlinearies of three derivatives of 2-amino-1,2,3-triazole with a ferrocenyl donor group and three different acceptor groups [51]. In those studies, the third-order nonlinear susceptibilities $\chi^{(3)}$ for the different molecules ranged from 0.23×10^{-11} esu up to 2.08×10^{-11} esu for nonlinear refraction experiments at 532 nm (nanosecond excitation) and between 0.10×10^{-11} and 0.13×10^{-11} esu for the Kerr response at 800 nm (femtosecond excitation). The maximum $\chi^{(3)}$ value reported by Rangel-Rojo et al. (reached under nanosecond excitation) is about three times larger than the value we measured for ATZQ, note however that in their experiments the mechanism originating the large nonlinearities was thermo-optic (and in consequence it implied a relatively slow nonlinear process) as the laser excitation (532 nm) fell within the absorption band. In contrast, the susceptibility measured for ATZQ ($\chi^{(3)} \sim 0.7 \times 10^{-11}$ esu) was not influenced by thermo-optic effects. It should be also noticed that HRS and THG are experiments in which the physical mechanism originating the second- and third-order nonlinearities are of electronic origin, i.e., second-harmonic and third-harmonic generation are a consequence of the nonlinear polarization produced in the molecular electronic configuration. In consequence, the nonlinear response measured for ATZQ has the attribute of being ultrarapid, a desirable characteristic for photonic applications.

CONCLUSIONS

In summary, we have characterized the first and second hyperpolarizabilities of ATZQ at infrared wavelength and with nanosecond excitation. The small heterocyclic-ring system conformed by the triazole and quinone moieties produced first and second hyperpolarizabilities as high as $\beta = 834 \times 10^{-30}$ esu and $\gamma = 3560 \times 10^{-36}$ esu, obtained through the detection of second-harmonic and third-harmonic generation, respectively. The nonlinearities are of electronic origin, due to an intramolecular electronic transfer process. This compound has the attribute of producing doped polymer thin films of high optical quality. The significant nonlinearities found for 2-amino-1,2,3-triazole derivatives are promising for NLO applications.

ACKNOWLEDGMENT

This work was supported by CONCyTEG (Project 07-04K662-080 A3) and by CONACyT (Project J49512 F). M.M.R. is thankful to Teresa de Jesus Palacios and Luis Ricardo Hernandez (UDLA) for support on NMR and X-ray diffraction experiments. The authors thank Rafael Espinosa for the film thickness measurements.

REFERENCES

[1] Prasad, P. N., & Williams, D. J. (1991). *Introduction to Nonlinear Optical Effects in Molecules and Polymers.* John & Wiley, New York.
[2] Nalwa, H. S., & Miyata, S. (Eds.). (1997). *Nonlinear Optics of Organic Molecules and Polymers.* CRC Pres, Boca Raton: Florida.
[3] Marder, S. R., Sohn, J. E., & Stucky, G. D. (Eds.). (1991). *Materials for Nonlinear Optics. ACS Symposium Series 455.* American Chemical Society: Washington, DC.
[4] Bredas, J. L., Adant, C., Tackx, P., & Persoons, A. (1994). *Chem. Rev.*, *94*, 243.
[5] Wolff, J. J., Siegler, F., Matschiner, R., & Wortmann, R. (2000). *Angew. Chem. Int. Ed. Engl.*, *39*, 1436.
[6] Long, N. J. (1995). *Angew. Chem. Int. Ed. Engl.*, *34*, 21.
[7] Cummings, S. C., Cheng, L.-T., & Eisenberg, R. (1997). *Chem. Mat.*, *9*, 440.
[8] Morrall, J. P., Dalton, G. T., Humphrey, M. G., & Samoc, M. (2008). *Adv. Organomet. Chem.*, *55*, 61.
[9] Marder, S. R., Perry, J. W., Tiemann, B. G., & Schaefer, W. P. (1991). *Organometallics*, *10*, 1896.
[10] Houlton, A., Miller, J. R., Silver, J., Jassim, N., Ahmet, M. J., Axon, T. L., Bloor, D., & Cross, G. H. (1993). *Inorg. Chim. Acta*, *205*, 67.
[11] Chou, S.-S. P., Hsu, G.-T., & Lin, H.-C. (1999). *Tetrahedron Lett.*, *40*, 2157.
[12] Whitaker, C. M., Patterson, E. V., Kott, K. L., & McMahon, R. J. (1996). *J. Am. Chem. Soc.*, *118*, 9966.
[13] Okada, A. S., Oikawa, H., & Nakanishi, H. (2000). *Chem. Mater.*, *12*, 1162.
[14] Briel, O., Sünkel, K., Krossing, I., Nöth, H., Schmälzlin, E., Meerholz, K., Bräuchle, C., & Beck, W. (1999). *Eur. J. Inorg. Chem.*, *1999*, 483.

[15] Garin, J., Orduna, J., Ruperez, J. I., Alcala, R., Villacampa, B., Sanchez, C., Martin, N., Segura, J. L., & Gonzalez, M. (1998). *Tetrahedron Lett.*, *39*, 3577.
[16] Herranz, M. A., Martin, N., Sanchez, L., Garin, J., Orduna, J., Alcala, R., Villacampa, B., & Sanchez, C. (1998). *Tetrahedron*, *54*, 11651.
[17] Glaser, R., & Chen, G. S. (1997). *Chem. Mater.*, *9*, 28.
[18] Zhang, J.-P., & Chen, X.-M. (2006). *Chem. Commun.*, 1689.
[19] Milton, N. G. N. (2001). *Neurotoxicology*, *22*, 767.
[20] Chicharro, M., Zapardiel, A., Bermejo, E., & Moreno, M. (2003). *Talanta*, *59*, 37.
[21] Fan, W.-Q., & Katritzky, A. R. (1996). "1,2,3-Triazoles". In: *Comprehensive Heterocyclic Chemistry*, 2nd edition. Katritzky, A. R., Rees, C. W., & Scriven, E. F. V. (Eds.), Pergamon: New York.
[22] Sun, D., & Watson, W. H. (1997). *J. Org. Chem.*, *62*, 4082.
[23] Sun, D., Krawiec, M., Campana, C. F., & Watson, W. H. (1997). *J. Chem. Cryst.*, *27*, 577.
[24] Bodige, S. G., Mendez-Rojas, M. A., & Watson, W. H. (1997). *J. Chem. Cryst.*, *29*, 931.
[25] Bodige, S. G., Mendez-Rojas, M. A., & Watson, W. H. (1999). *J. Chem. Cryst.*, *29*, 57.
[26] Rangel-Rojo, R., Stranges, L., Kar, A. K., Mendez-Rojas, M. A., & Watson, W. H. (2003). *Opt. Commun.*, *203*, 385.
[27] Rangel-Rojo, R., Kimura, K., Matsuda, H., Mendez-Rojas, M. A., & Watson, W. H. (2003). *Opt. Commun.*, *228*, 181.
[28] Méndez-Rojas, M. A., Bodige, S. G., Ejsmont, K., & Watson, W. H. (2001). *J. Chem. Cryst.*, *31*, 257.
[29] Méndez-Rojas, M. A., Bodige, S. G., Ejsmont, K., & Watson, W. H. (1999). *J. Chem. Cryst.*, *29*, 1225.
[30] Parent, M., Mongin, O., Kamada, K., Katana, K., & Blanchard-Desce, M. (2005). *Chem. Commun.*, 2029.
[31] Westlund, R., Glimsdal, E., Lindgren, M., Vestberg, R., Hawker, C., Lopesd, C., & Malmström, E. (2008). *J. Mater. Chem.*, *18*, 166.
[32] Grice, A. W., Tajbakhsh, A. R., Burn, P. L., Bradley, D. D., & (Zakya, H. Ed.) SPIE Proceedings. (1997). Vol. 3148, San Diego, paper 3148–23.
[33] Zhao, X.-X., Ma, J.-P., Dong, Y.-B., Huang, R.-Q., & Lai, T. (2007). *Crystal Growth & Design*, *7*, 1058.
[34] Matulková, I., Němec, I., Císařová, I., Němec, P., & Mička, Z. (2007). *J. Mol. Struct.*, *834–836*, 328.
[35] Bruker Analytical X-ray Systems. (2000). *SMART: Bruker Molecular Analysis Research Tool V.5.618*.
[36] Bruker Analytical X-ray Systems. (2001). *SAINT-NT version 6.04*.
[37] (a)Sheldrick, G. M. (1986). *SHELXS-86,* Program for Crystal Structure Solution; University of Göttingen: Germany; (b) SHELXTL-NT. (2000). Version 6.10, Bruker Analytical X-ray Systems.
[38] Farrugia, L. J. (1997). *J. Appl. Crystallogr.*, *32*, 837.
[39] Farrugia, L. (1997). *J. Appl. Crystallogr.*, *30*, 565.
[40] *Mercury*, version 1.1.2; Cambridge Crystallographic Data Centre: Cambridge, U.K., 2002.
[41] Hendrickx, E., Clays, K., & Persoons, A. (1998). *Acc. Chem. Res.*, *31*, 675.
[42] Wang, X. H., West, D. P., McKeown, N. B., & King, T. A. (1998). *J. Opt. Soc. Am. B*, *15*, 1895.
[43] Becke, A. D.. (1993). *J. Chem. Phys.*, *98*, 5648.
[44] Gaussian 98, Revision A.6, Frisch, M. J., Trucks, G. W., Schlegel, H. B., Scuseria, G. E., Robb, M. A., Cheeseman, J. R., Zakrzewski, V. G., Montgomery, Jr., J. A.,

Stratmann, R. E., Burant, J. C., Dapprich, S., Millam, J. M., Daniels, A. D., Kudin, K. N., Strain, M. C., Farkas, O., Tomasi, J., Barone, V., Cossi, M., Cammi, R., Mennucci, B., Pomelli, C., Adamo, C., Clifford, S., Ochterski, J., Petersson, G. A., Ayala, P. Y., Cui, Q., Morokuma, K., Malick, D. K., Rabuck, A. D., Raghavachari, K., Foresman, J. B., Cioslowski, J., Ortiz, J. V., Stefanov, B. B., Liu, G., Liashenko, A., Piskorz, P., Komaromi, I., Gomperts, R., Martin, R. L., Fox, D. J., Keith, T., Al-Laham, M. A., Peng, C. Y., Nanayakkara, A., Gonzalez, C., Challacombe, M., Gill, P. M. W., Johnson, B., Chen, W., Wong, M. W., Andres, J. L., Gonzalez, C., Head-Gordon, M., Replogle, E. S., & Pople, J. A. Gaussian, Inc., Pittsburgh PA, 1998.

[45] Chui, T. W., & Wonga, K. Y. (1998). *J. Chem. Phys.*, *109*, 1391.

[46] Morrison, I. D., Denning, R. G., Laidlaw, W. M., & Stammers, M. A. (1996). *Rev. Sci. Instrum.*, *67*, 1445.

[47] Rao, Y., Guo, X.-M., Tao, Y.-S., & Wang, H.-F. (2004). *J. Phys. Chem. A*, *108*, 7977.

[48] Kajzar, F., & Messier, J. (1985). *Phys. Rev. A*, *32*, 2352.

[49] Ramos-Ortiz, G., Maldonado, J. L., Meneses-Nava, M. A., Barbosa-García, O., Olmos-López, M., & Cha, M. (2007). *Optical Materials*, *10*, 636.

[50] Rojo, G., Angulló-López, F., Cabezón, B., Torres, T., Brasselet, S., Ledoux, I., & Zyss, J. (2000). *J. Phys. Chem. B*, *104*, 4295.

[51] (a) Torres-Torres, C., Khomenko, A. V., Tamayo-Rivera, L., Rangel-Rojo, R., Mao, Y., & Watson, W. H. (2008). *Optics Commun.*, *281*, 3369; (b) Tamayo-Rivera, L., Rangel-Rojo, R., Mao, Y., & Watson, W. H. (2008). *Optics Commun.*, 281, 5239.